



Experimental and Theoretical Studies on the Molecular Structure, FT-IR, NMR, HOMO, LUMO, MESP, and Reactivity Descriptors of (*E*)-1-(2,3-Dihydrobenzo[*b*][1,4]dioxin-6-yl)-3-(3,4,5-trimethoxyphenyl)prop-2-en-1-one

**RAHUL ASHOK SHINDE^{1,2}, VISHNU ASHOK ADOLE^{2*},
BAPU SONU JAGDALE^{1,2} and THANSING BHAVSING PAWAR¹**

¹Department of Chemistry, Mahatma Gandhi Vidyamandir's Loknete Vyankatrao Hiray Arts, Science and Commerce College Panchavati (Affiliated to SP Pune University, Pune), Nashik-422 003, India.

²Department of Chemistry, Mahatma Gandhi Vidyamandir's Arts, Science and Commerce College (Affiliated to Savitribai Phule Pune University, Pune), Manmad-423104, India.

Abstract

The present research deals with the synthesis, characterization and density functional theory (DFT) study of (*E*)-1-(2,3-dihydrobenzo[*b*][1,4]dioxin-6-yl)-3-(3,4,5-trimethoxyphenyl)prop-2-en-1-one (DTMPP). For the computational investigation, DFT method at B3LYP/6-311++G(d,p) basis set has been used. Herein, structural properties like molecular structure, bond lengths, and bond angles of the DTMPP have been explored. The all-important examination of the electronic properties; HOMO and LUMO energies were studied by the time-dependent DFT (TD-DFT) method. The experimental and theoretical spectroscopic investigation on FT-IR, ¹H NMR, and ¹³C NMR has been unveiled in the present research. To study the chemical behaviour of the DTMPP, Mulliken atomic charges, molecular electrostatic surface potential, and reactivity descriptors have been explored. The dipole moment of the DTMPP is 1.27 Debye with C₁ point group symmetry and -1225.77 a.u. E(B3LYP) energy. The most electropositive carbon and hydrogen atoms in the DTMPP are C₁₄ and H₂₇ respectively. The C₁-C₆ bond is the longest (1.4089 Å) C=C bond in the DTMPP. The oxygen atom O₃₃ is having short contact interaction with the hydrogen atom H₄₄ with a distance of 3.3258 Å. The molecular electrostatic potential plot predicts the positive electrostatic potential is around hydrogen atoms. The FT-IR assignments were made by comparing the experimental



Article History

Received: 10 May 2020
Accepted: 01 June 2020

Keywords:

(*E*)-1-(2,3
Dihydrobenzo[*b*][1,4
Dioxin-6-yl)-3-(3,4,5-
Trimethoxyphenyl)Prop-
2-En-1-One,
B3lyp/6-311++G(D,P);
Dft;
Molecular Structure;
Molecular Electrostatic
Surface Potential.

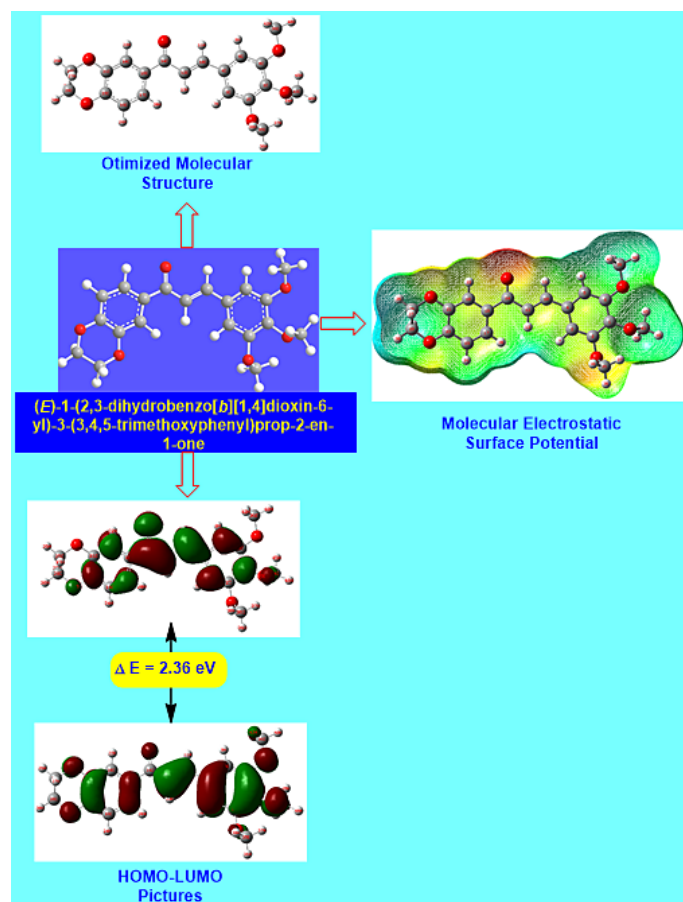
CONTACT Vishnu Ashok Adole ✉ vishnuadole86@gmail.com 📍 Department of Chemistry, Mahatma Gandhi Vidyamandir's Arts, Science and Commerce College (Affiliated to Savitribai Phule Pune University, Pune), Manmad-423104, India.



© 2020 The Author(s). Published by Oriental Scientific Publishing Company

This is an Open Access article licensed under a Creative Commons Attribution-NonCommercial-ShareAlike 4.0 International License
Doi: <http://dx.doi.org/10.13005/msri.17.special-issue1.07>

FT-IR absorption peaks with the scaled frequencies obtained using DFT method. Furthermore, some valuable insights on thermochemical data are obtained using the harmonic frequencies at same basis set.



Graphical Abstract

Introduction

Chalcones are open chain compounds that are considered as pathway to naturally occurring compounds flavonoids and isoflavonoids. Many chalcones and their hybrid derivatives are synthesized in last two decades.¹⁻⁵ Both natural and synthetic versions of chalcones display enormous applications in pharmacological field.⁶⁻¹⁰ Structurally, chalcones are 1,3-diaryl-2-propen-1-ones and exist as *cis* and *trans* forms; latter being thermodynamically more stable is more predominant. Chalcones are considered as vital intermediates to synthesize wide variety of heterocyclic compounds with broad-spectrum of biological activities.¹¹⁻¹⁶

The extraordinary pharmacological profile of chalcones and their hybrid derivatives include anticancer,¹⁷⁻²⁰ anti-tubercular,^{21,22} antibacterial,²³⁻²⁶ anti-HIV,²⁷⁻³⁰ antimalarial,³¹⁻³⁴ antioxidants,³⁵⁻³⁷ antiviral,³⁸⁻⁴⁰ antifungal,⁴¹⁻⁴⁵ cardiovascular,^{46,47} antitumor,⁴⁸⁻⁵⁰ antiulcer,⁵¹ anticonvulsant,^{52, 53} anti-inflammatory,⁵⁴⁻⁵⁹ activities. Besides, chalcones also exhibit applications in the field of solar cells,⁶⁰ photo-alignment layer of liquid crystal display⁶¹ optoelectronics,⁶² corrosion and photo crosslinking,⁶³ and nonlinear optical materials.⁶⁴⁻⁶⁷ All these noteworthy aspects about chalcones make them widely studied and synthesized compounds in the fields of science. Green chemistry has advanced

in recent years and many methods have been modified in order to increase the reaction efficiency and reduce waste material.⁶⁸⁻⁷⁵ Many methods have been accounted for the synthesis of chalcones; but still, the most common method which is being used for the synthesis of chalcones is Claisen-Schmidt condensation.⁵

The field of DFT has attracted researchers due to its wide applications in structural chemistry. Many vital structural parameters could be anticipated with the help of DFT. The molecular properties like molecular structure, bond lengths, and bond angles along with spectroscopic properties like UV-Visible, FT-IR, Raman, and NMR have been largely explored by using DFT method using proper basis set.⁷⁶⁻⁸⁰ To investigate all these important aspects DFT has been employed to study the molecules like 2-arylidene indanone,⁸¹ (E)-1-(5-bromo-2-hydroxybenzylidene) semicarbazide,⁸² (E)-1-(4-bromobenzylidene) semicarbazide,⁸³ 3,5-Difluoroaniline,⁸⁴ (E)-3-[4-(pentyloxy)phenyl]-1-phenylprop-2-en-1-one,⁸⁵ N-phenylbenzenesulfonamide,⁸⁶ 3-ethynylthiophene,⁸⁷ SnO₂ nanopowder,⁸⁸ 2-Thienylboronic acid,⁸⁹ 3,5-dimethyl-4-methoxybenzoic acid,⁹⁰ 4-hydroxy-3-methoxycinnamaldehyde,⁹¹ 3-alkyl-4-[3-methoxy-4-(4-methylbenzoyl)benzylideneamino]-4,5-dihydro-1H-1,2,4-triazol-5-ones,⁹² 5-bromo-2-ethoxyphenylboronic acid,⁹³ 5-benzyl 2-thiohydantoin,⁹⁴ Chlorfenson,⁹⁵ sulfamethoxazole,⁹⁶ terephthalic acid,⁹⁷ 1-phenyl-2-nitropropene,⁹⁸ 1-bromo-4-nitrobenzene,⁹⁹ 4-bromo-1-(ethoxycarbonyl)piperidine-4-carboxylic acid,¹⁰⁰ 2-Bromo-1H-Benzimidazol,¹⁰¹ dansyl chloride¹⁰² etc. In view of all these discussed vital aspects of the modern times, herein I wish report combined experimental and theoretical studies on the molecular structure, FT-IR, NMR, HOMO, LUMO, MESP surface, and reactivity descriptors of (E)-1-(2,3-dihydrobenzo[b][1,4]dioxin-6-yl)-3-(3,4,5-trimethoxyphenyl)prop-2-en-1-one. In the present research, DFT investigation of the optimized

molecular structure, bond length, bond angle, Mulliken atomic charges and harmonic vibrational frequencies have been investigated. The important parameters such as total energy, HOMO-LUMO energies, charge distribution, ionization potential, electron affinity, electronegativity, global softness, absolute hardness, global electrophilicity index, chemical potential, charge *transfer* have been studied using 6-311++G(d,p) basis set.

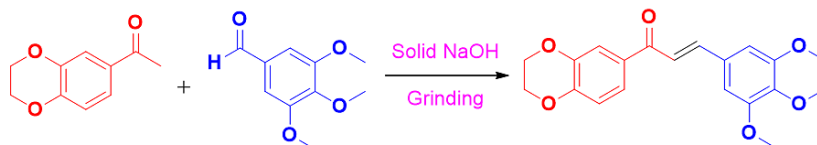
Materials and Methods

General Remarks

The chemicals (Make- Sigma Aldrich, SD Fine Pvt. Ltd., and Avra synthesis) were purchased from local distributor, Nashik with a high purity. The FT-IR spectrum of the DTMP was recorded on Shimadzu spectrometer using a KBr disc technique. The NMR experiment was performed on sophisticated multinuclear FT-NMR Spectrometer (500 MHz) model Advance-II (Bruker). The compound was dissolved in chloroform-d. Chemical shifts were reported in ppm relative to tetramethylsilane (TMS). The reaction was followed by using thin-layer chromatography on Merck Aluminium TLC plate, silica gel coated with fluorescent indicator F254. All the glass apparatus were cleaned and dried in oven prior to use.

Experimental Procedure for the Synthesis of the DTMP

The DTMP was synthesized using Claisen-Schmidt condensation reaction. In a typical synthesis method, 1-(2,3-dihydrobenzo[b][1,4]dioxin-6-yl)ethan-1-one (1, 10 mmol) and 3,4,5-trimethoxybenzaldehyde (1, 10 mmol) were mixed and added into mortar and pestle. Equimolar amount of solid NaOH was added. Then the alkaline mixture was grinded until formation of the product. After completion of the reaction (monitored by TLC), the reaction was quenched by pouring onto the crushed ice. It was then acidified by dilute HCl, filtered, dried and recrystallized to give pure crystals of the DTMP. The reaction is presented in the Scheme 1.



Scheme 1: Synthesis of the DTMP

Computational Details

For DFT calculations Gaussian 03(W) program package is used. All the calculations are performed at optimized by using DFT/B3LYP method using 6-311++G (d,p) basis set. Gauss View 4.1 molecular visualization program is used to visualize the optimized structure. The molecular structure is optimized at the same level. The structural parameters like bond length and bond angles,

Mulliken atomic charges, molecular electrostatic surface potential, thermochemical data for the DTMP were determined. The absorption wavelength (λ in nm), oscillator strength (f), and *transitions* of DTMP were computed at TD-B3LYP/6-311++G (d,p) level of theory for B3LYP/6-311G++(d,p) optimized geometry. All the DFT calculations were performed for the optimized molecular structure in the gas phase.

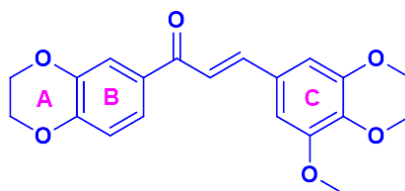


Fig.1: Structure of DTMP (with ring labeling)

Results and Discussion

Spectral Analysis of the DTMP

The DTMP was characterized by spectral methods like FTIR, ^1H NMR, and ^{13}C NMR. The structure with ring labelling is depicted in Figure 1. The FT-IR spectrum is depicted in Figure 2, ^1H NMR in Figure 3, and ^{13}C NMR in Figure 4. In ^1H NMR spectrum, the DTMP has displayed all expected signal. The two protons situated at the C=C (alkene framework) are mutually coupled to each other by a

coupling constant, $J = 15.6$ Hz which suggests the stereochemistry of an olefinic double bond is *trans*. All other signals in ^1H NMR spectrum are ideally matching with structural arrangement of the DTMP. In ^{13}C NMR spectrum, the very important carbon signal is at 188.49 δ which is ascribed to ketonic carbonyl carbon. Other carbon signals are also correctly matching. The FT-IR spectral assignments were discussed in latter section.

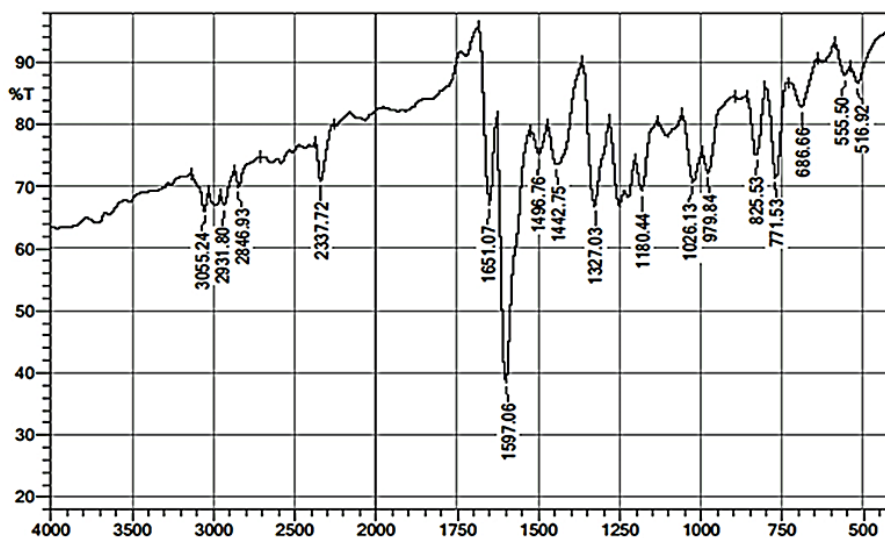
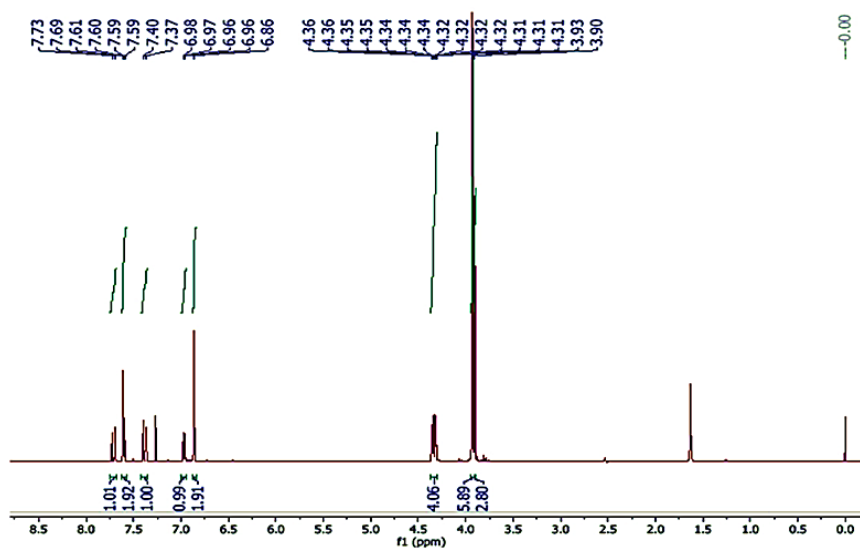
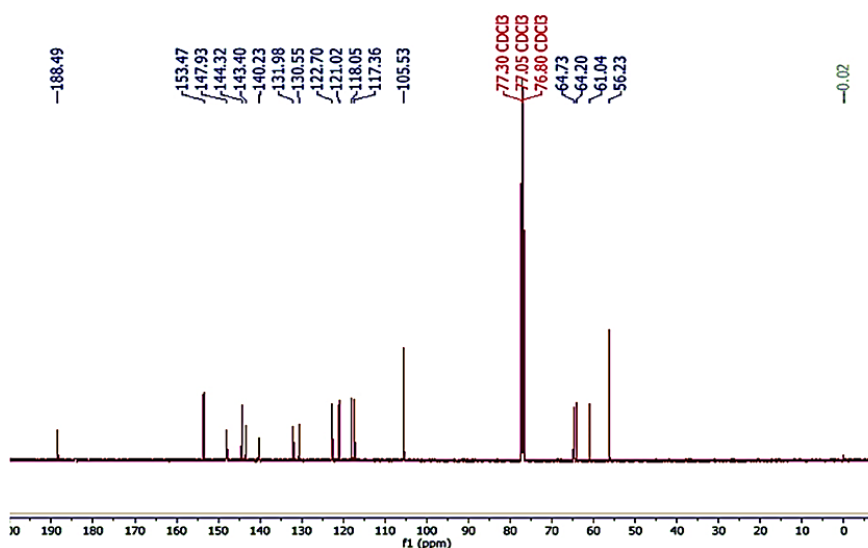


Fig.2: FT-IR spectrum of DTMP

Fig.3: ¹H NMR spectrum of DTMPFig.4: ¹³C NMR spectrum of DTMP

(E)-1-(2,3-dihydrobenzo[*b*][1,4]dioxin-6-yl)-3-(3,4,5-trimethoxyphenyl)prop-2-en-1-one

FT-IR (cm⁻¹, KBr) 3055.24, 2931.80, 2846.93, 2337.72, 1651.07, 1597.06, 1496.76, 1442.75, 1327.03, 1180.44, 1026.13, 979.84, 825.53, 771.53, 686.66, 555.50, 516.92; ¹H NMR (500 MHz, CDCl₃) δ 3.90 (s, 3H), 3.93 (s, 6H), 4.37 – 4.30 (m, 4H), 6.86 (s, 2H), 6.99 – 6.94 (m, 1H), 7.38 (d, *J* = 15.6 Hz, 1H), 7.60 (m, 2H), 7.71 (d, *J* = 15.6 Hz, 1H); ¹³C NMR (126 MHz, CDCl₃) δ 56.23, 61.04, 64.20,

64.73, 105.53, 117.36, 118.05, 121.02, 122.70, 130.55, 131.98, 140.23, 143.40, 144.32, 147.93, 153.47, 188.49.

DFT Study

Molecular Structure, Bond Length, Bond Angle Study

The optimized molecular structure of the DTMP has been presented in the Figure 5. Optimized bond lengths and bond angles of DTMP at B3LYP/6-

311++G(d,p) are presented in Table 1 and Table 2 respectively. The DTMP possess aromatic C=C bond lengths from 1.39 Å to 1.40 Å. The alkene (C10=C12) bond is 1.3447 Å long and the carbonyl (C14=O15) bond is 1.2249 Å in length. The C1-C6 bond is the longest (1.4089 Å) C=C bond in the DTMP. The oxygen atom O33 is having short contact interaction with the hydrogen atom H44 with

a distance of 3.3258 Å. The dipole moment of the DTMP is 1.27 Debye with C1 point group symmetry and -1225.77 a.u. E(B3LYP) energy. The bond angles C23-O32-C28, C21-O31-C25, C25-C28-O32, and C28-C25-O31 are 114.3374, 113.7255, 110.1429, and 110.0488° respectively. Other bond length and bond angle data is also in good agreement.

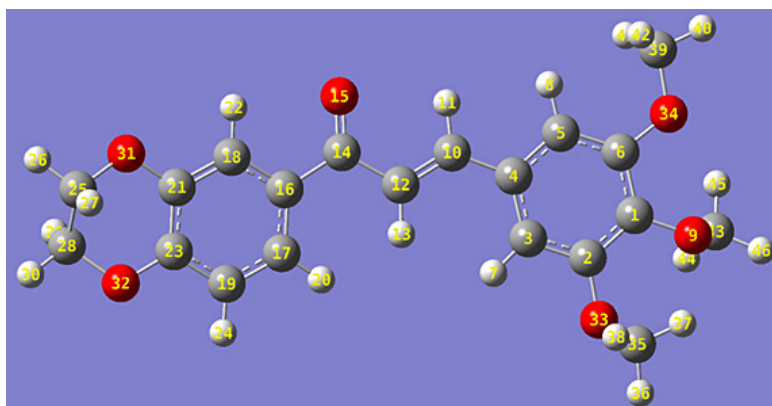


Fig.5: Optimized Molecular Structure of the DTMP

Table 1: Optimized bond lengths of DTMP at B3LYP/6-311++G(d,p)

Bond lengths (Å)					
C1-C2	1.403	C12-C14	1.4843	C25-C28	1.5166
C1-C6	1.4089	C14-O15	1.2249	C25-O31	1.428
C1-C9	1.3684	C14-C16	1.4986	C28-H29	1.096
C2-C3	1.3905	C16-C17	1.4034	C28-H30	1.0904
C2-O33	1.3712	C16-C18	1.4002	C28-O32	1.4321
C3-C4	1.3999	C17-C19	1.3882	O33-C35	1.4344
C3-H7	1.0822	C17-H20	1.0813	O33-H44	3.3258
C4-C5	1.4066	C18-C21	1.3848	O34-C39	1.4224
C4-C10	1.4599	C18-H22	1.0824	C35-H36	1.0896
C5-C6	1.3927	C19-C23	1.393	C35-H37	1.0911
C5-H8	1.0815	C19-H24	1.0833	C35-H38	1.0957
C6-C34	1.3626	C21-C23	1.4073	C39-H40	1.0886
O9-C43	1.435	C21-C31	1.3731	C39-H41	1.0954
C10-H11	1.0874	C23-C32	1.3667	C39-H42	1.0951
C10-C12	1.3447	C25-H26	1.0905	C43-H44	1.0944
C12-H13	1.0817	C25-H27	1.0968	C43-H45	1.0921
-	-	-	-	C43-H44	1.0896

**Table 2: Optimized bond angles of DTMP
at B3LYP/6-311++G(d,p)**

Bond angles (°)					
C2-C1-C6	119.203	C15-C14-C16	119.9414	C25-C28-O32	110.1429
C2-C1-O9	119.654	C14-C16-C17	124.1855	C29-C28-H30	109.2448
C6-C1-O9	121.1151	C14-C16-C18	117.105	C29-C28-O32	109.4186
C1-C2-C3	120.5619	C17-C16-C18	118.7092	H30-C28-O32	106.2509
C1-C2-O33	120.8758	C16-C17-C19	120.5274	C21-O31-C25	113.7255
C3-C2-O33	118.4956	C16-C17-H20	121.0765	C23-O32-C28	114.3374
C2-C3-C4	120.6212	C19-C17-H20	118.3819	C2-O33-C35	115.9901
C2-C3-H7	117.6039	C16-C18-C21	121.0782	C6-O34-C39	118.3398
C4-C3-H7	121.7635	C16-C18-H22	119.3046	O33-C35-H36	105.9214
C3-C4-C5	118.8277	C21-C18-H22	119.617	O33-C35-H37	111.2063
C3-C4-C10	123.211	C17-C19-C23	120.381	O33-C35-H38	110.4968
C5-C4-C10	117.9597	C17-C19-H24	121.508	H36-C35-H37	109.8833
C4-C5-C6	120.9288	C23-C19-H24	118.1089	H36-C35-H38	109.2885
C4-C5-H8	118.6506	C18-C21-C23	119.7267	H37-C35-H38	109.9568
C6-C5-H8	120.4205	C18-C21-O31	118.7515	O34-C39-H40	105.7252
C1-C6-C5	119.851	C23-C21-O31	121.5209	O34-C39-H41	111.5441
C1-C6-O34	115.4102	C19-C23-C21	119.5634	O34-C39-H42	111.3529
C5-C6-O34	124.7374	C19-C23-O32	118.4071	H40-C39-H41	109.3594
C1-O9-C43	115.3767	C21-C23-O32	122.0292	H40-C39-H42	109.3165
C4-C10-H11	116.1274	H26-C25-H27	109.1376	H41-C39-H42	109.4515
C4-C10-C12	128.0884	H26-C25-C28	111.3025	O9-C43-H44	110.546
C11-C10-C12	115.7842	H26-C25-O31	106.4255	O9-C43-H45	110.8797
C10-C12-H13	120.8568	H27-C25-C28	110.1061	O9-C43-H46	106.0459
C10-C12-C14	119.9991	H27-C25-O31	109.746	H44-C43-H45	110.1828
H13-C12-C14	119.1389	C28-C25-O31	110.0488	H44-C43-H46	109.5231
C12-C14-O15	120.986	C25-C28-H29	110.1292	H45-C43-H46	109.573
C12-C14-C16	119.0706	C25-C28-H30	111.5645	-	-

Mulliken Atomic Charges and MESP Analysis

The Mulliken nuclear charges depend on the electron density. The charge conveyance on the molecule has a fundamental job in the field of quantum mechanical calculations for the molecular systems. The Mulliken atomic charges of the DTMP are determined by DFT/B3LYP method with a 6-311++G(d,p) basis set are given in Table 3 and the pictorial presentation in Figure 6. Mulliken nuclear charges

uncover that all the hydrogen atoms have a net positive charge but H40 atom has a more positive charge (0.131720) than other hydrogen atoms and in this way highly acidic. The C14 atom has the highest net positive charge (0.258693) and the C16 is the most electronegative carbon (-0.172547). Molecular electrostatic potential surface (MESP) is the three dimensional portrayal of the charge distributions in the molecules.

Table 3: Mulliken atomic charges of DTMP

Atom	Charge	Atom	Charge
1 C	0.128758	24 H	0.101714
2 C	0.137002	25 C	-0.039861
3 C	-0.028609	26 H	0.122036

4 C	-0.070414	27 H	0.125682
5 C	-0.078696	28 C	-0.033079
6 C	0.186623	29 H	0.128327
7 H	0.084342	30 H	0.121675
8 H	0.105487	31 O	-0.347037
9 O	-0.373934	32 O	-0.347018
10 C	-0.022806	33 O	-0.370983
11 H	0.108857	34 O	-0.352687
12 C	-0.183709	35 C	-0.112558
13 H	0.108190	36 H	0.112704
14 C	0.258693	37 H	0.126112
15 O	-0.332374	38 H	0.093758
16 C	-0.172547	39 C	-0.134310
17 C	-0.042463	40 H	0.131720
18 C	-0.030810	41 H	0.115056
19 C	-0.102820	42 H	0.117146
20 H	0.090052	43 C	-0.106943
21 C	0.156429	44 H	0.103928
22 H	0.117097	45 H	0.116446
23 C	0.171490	46 H	0.114333

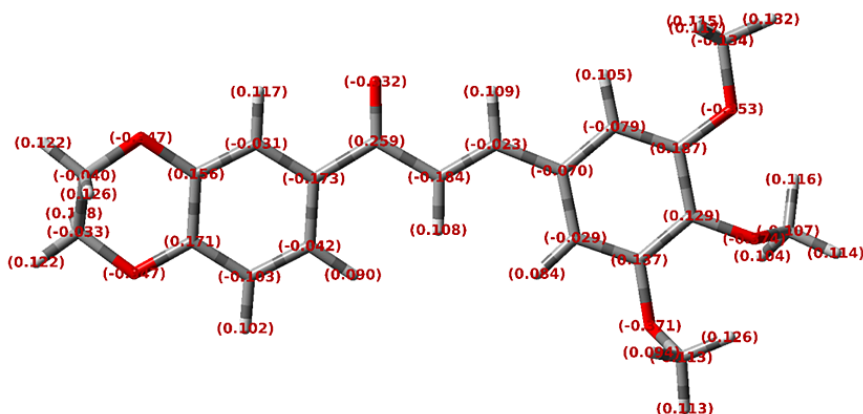


Fig.6: Mulliken atomic charges of DTMPP

The MESP diagram plotted by employing 6-311++G(d,p) basis set and depicted in Figure 7.⁸¹ Over the span of recent years, the molecular electrostatic potential has risen as a persuading tool for exploring molecular interactions. In current science, it has been adequately associated with a wide assortment of biological and chemical platforms. The vital aspects such as nucleophilic and electrophilic reactivity sites, solvent interactions, hydrogen-bonding phenomenon, and non-classical interactions could be anticipated by studying MESP plots. MESP fundamentally used to point out the

reactive sites of molecules that enable us to foresee how one molecule can interface with others. The red and yellow colours in the MESP plot indicate the region of high electron density and therefore linked with electrophilic reactivity. On the contrary, the blue colours reveal low electron density and thus susceptible to nucleophilic attacks. The green colours are areas of zero potential. The MESP plot of the DTMPP suggest that the electrophilic attacks are feasible at both aromatic rings; However, ring C is more prone for the attack of electrophiles. The positive potential is around hydrogen atoms.

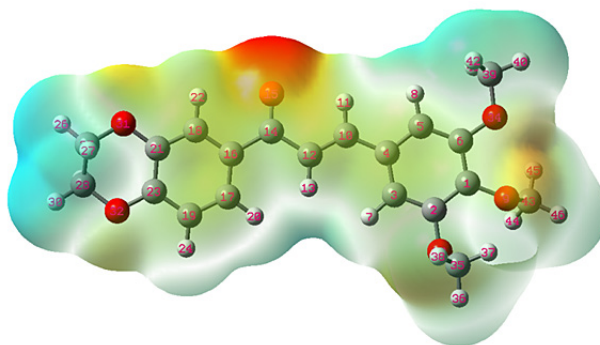


Fig.7: Molecular electrostatic potential surface of DTMP

HOMO, LUMO, Reactivity Descriptors, and Absorption Energies

The pictorial representation of the frontier molecular orbitals (FMOs) has depicted in Figure 8. The FMOs, HOMO and LUMO are crucial to evaluate the reactivity and the stability of the molecules. More importantly HOMO is connected to the electron donating capacity and the LUMO is connected with electron-accepting ability. The smaller HOMO-LUMO band gap suggests more stability. Thus, the HOMO-LUMO energy gap is the most important indicator of the kinetic stability of molecules. The

HOMO and LUMO energies are -6.023 and -2.280 eV individually. The reduction in the HOMO-LUMO energy gap prompts an expansion in polarizability, flexibility, and electron *transport* in a molecule. The HOMO and LUMO energies are extremely essential as they are linked to ionization enthalpy and electron affinity individually. The HOMO in the DTMP is principally located at ring B and C. The LUMO is basically situated at the enone part of the unsaturated system. The energy gap in the DTMP is 3.783 eV which reveals inevitable charge *transfer* phenomena taking place within the molecule.

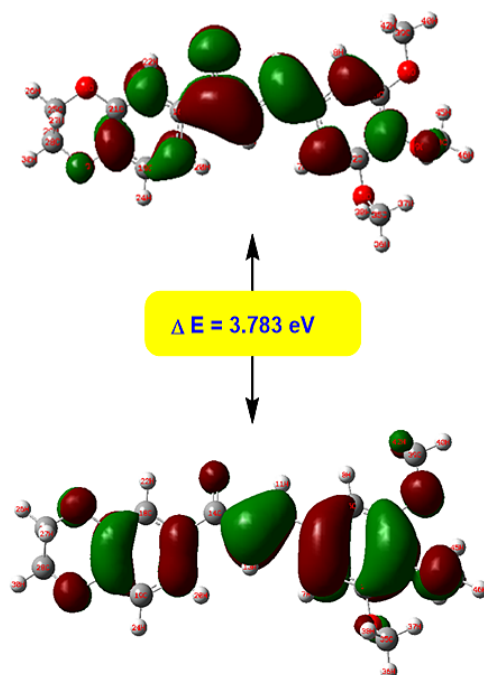


Fig.8: HOMO-LUMO pictures of DTMP

With the help of Koopmans's theorem, various reactivity descriptors are calculated. The important parameters such as total energy, HOMO-LUMO energies, charge distribution, electron affinity, ionization potential, global softness, absolute hardness, electronegativity, global electrophilicity index, chemical potential, and charge transfer are evaluated. The ionization potential (I) and the electron affinity (A) values are 6.023 and 2.280 eV respectively. The electronegativity value in electron volt is 4.15 eV. The absolute hardness (η) is 1.89 eV and the global softness (σ) is 0.53 eV^{-1} . These values indicate that the molecule DTMPP is softer in nature. The global electrophilicity index (ω) is 4.55 eV which tells that the DTMPP is a good electrophile. The chemical potential (μ) value is -4.15 eV in the

DTMPP. The maximum charge transfer (ΔN_{max}) in the DTMPP is 2.19 eV.

The absorption wavelength (λ in nm), oscillator strength (f), and transitions of DTMPP were computed at TD-B3LYP/6-311++ G(d,p) level of theory for B3LYP/6-311G ++(d,p) optimized geometry in gas phase presented in the Table 4. The UV-Visible spectrum was computed for six excited states. The first excited state absorption wavelength is 375.83 nm with excitation energy of 3.2990 eV and oscillator strength (f), 0.0035. With increase in the number of excited state, there is decrease in the absorption wavelength and increase in the excitation energy.

Table 4: Absorption energies (λ in nm), Oscillator strength (f), and transitions of DTMPP computed at TD-B3LYP/6-311G++(d,p) level of theory for B3LYP/6-311G ++(d, p) optimized geometry in gas phase

Sr. No.	Absorption Wavelength (nm)	Excitation energy (eV)	Excited state	Oscillator strength (f)
1	375.83	3.2990	1	0.0035
2	363.45	3.4113	2	0.6667
3	340.53	3.6409	3	0.0441
4	325.29	3.8115	4	0.1847
5	311.35	3.9821	5	0.0338
6	265.39	4.6718	6	0.0812

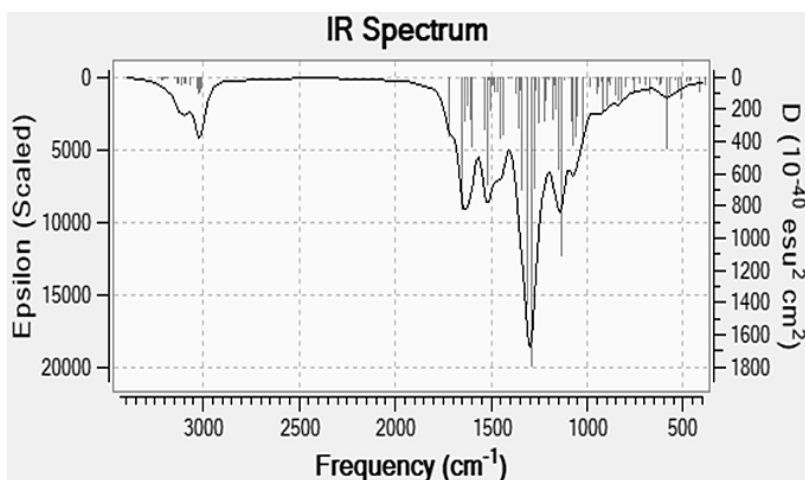


Fig.9: Theoretical IR spectrum of DTMPP

Vibrational Assignments and Thermochemical Study

The vibrational assignments for the DTMP were made by comparing experimental IR spectrum with the theoretical IR spectrum. The DFT based IR absorption values are slightly higher, therefore a scaling factor of 0.96 is used.⁶¹ A Comparison between selected theoretical and experimental vibrational assignments has been made and presented in Table 5. The DTMP contains 46 atoms; therefore, it shows 132 fundamental modes of vibrations. Results indicate that there is ideal matching between experimental and theoretical vibrational peaks. The theoretical IR spectrum is given in Figure 9. The DTMP has experimental carbonyl vibrational stretching frequency at 1651.07

cm⁻¹. The C=C of enone framework has stretching absorption peak at 1597.06 cm⁻¹. The peak at 3055.24 cm⁻¹ is due to stretching of C12-H bond, asymmetric stretching of C17-H-C19-H and C39-H2 bonds. The IR peak at 1442.75 cm⁻¹ corresponds to scissoring vibration of C39-H2 bond. The vibrational peak at 1327.03 cm⁻¹ is due to wagging vibrations of C25-H₂ and C28-H₂ bonds. The IR value 1180.44 cm⁻¹ is due to in plane bending vibrations of C17-H, C18-H, and C19-H bonds. The out of plane bending vibration of C5-H bond is observed at 825.53 cm⁻¹. The absorption peak 555.50 cm⁻¹ is ascribed to deformation vibrations of ring A, B, and ring C. Other vibrational assignments were also correctly made using theoretical IR spectrum.

Table 5: Comparison between selected experimental and theoretical vibrational assignments calculated at 6-311++G(d,p) level

Mode	Computed frequencies (cm-1)	IR Intensity (km mol-1)	Observed frequencies (cm-1)	Assignments
127	3059.26	5.01	3055.24	v C12-H + v asym C17-H-C19-H
118	2944.62	31.79	2931.80	v asym C39-H ₂
113	2887.07	51.43	2846.93	v sym C39-H ₂
112	1648.18	156.75	1651.07	v C=O
111	1583.68	338.02	1597.06	v C10=C12
106	1471.56	124.61	1496.76	v C=C (ring B)
102	1444.08	77.89	1442.75	v scis C39-H ₂
90	1337.20	1.59	1327.03	ω C25-H ₂ + ω C28-H ₂
85	1259.33	462.73	-	t C25-H ₂
83	1238.51	28.43	-	ρ C17-H-C19-H
78	1176.00	81.98	1180.44	β C17-H + β C18-H + β C19-H
65	1030.44	113.60	1026.13	v C25-O31
62	983.50	100.86	979.84	def ring C
51	815.11	24.10	825.53	γ C5-H
49	790.41	31.37	771.53	ω C17-H-C19-H
44	694.67	5.74	686.66	def ring B
38	559.07	65.24	555.50	def ring A + def ring B + def ring C

v- stretching; sym- symmetric; asym- asymmetric; def- deformation; scis- scissoring β- In-plane bending; γ- out of plane bending; ρ- rocking; t- twisting, ω -wagging

The thermochemistry data obtained for the DTMP from the DFT method at B3LYP/6-311++G (d,p) level is presented in Table 6. In the present study, E_{total}[†]

Heat capacity at constant volume, total entropy S, zero point vibrational energy and rotational constants have been evaluated from harmonic vibrational

frequencies. The total thermal energy is 244.365 kcal mol⁻¹. The total entropy is 178.630 cal mol⁻¹K⁻¹; out of which *translational* freedom is 43.504, rotational is 36.445, and the vibrational is 98.681 cal mol⁻¹K⁻¹. The

zero point vibrational energy is 228.84140 Kcal mol⁻¹. The information uncovered in this could be helpful for the further evaluation of the other thermodynamic properties.

Table 6: Thermochemical information of DTMPP

Parameter	Value
E total (kcal mol ⁻¹)	244.365
Translational	0.889
Rotational	0.889
Vibrational	242.587
Heat Capacity at constant volume, Cv (cal mol ⁻¹ K ⁻¹)	91.704
Translational	2.981
Rotational	2.981
Vibrational	85.742
Total entropy S (cal mol ⁻¹ K ⁻¹)	178.630
Translational	43.504
Rotational	36.445
Vibrational	98.681
Zero point Vibrational Energy Ev ₀ (Kcal mol ⁻¹)	228.84140
Rotational constants (GHZ)	0.53604
	0.06036
	0.05497

Conclusion

In outline, the current research deals with the synthesis, characterization and DFT study of (*E*)-1-(2,3-dihydrobenzo[*b*][1,4]dioxin-6-yl)-3-(3,4,5-trimethoxyphenyl)prop-2-en-1-one (DTMPP). For the computational investigation, DFT method at B3LYP/6-311++G(d,p) basis set has been used.

- Structural properties like molecular structure, bond lengths, and bond angles of the DTMPP have been investigated. The DTMPP has aromatic C=C bond lengths from 1.39 Å to 1.40 Å. The alkene (C10=C12) bond is 1.3447 Å long and the carbonyl (C14-O15) bond is 1.2249 Å in length. The C1-C6 bond is the longest (1.4089 Å) C=C bond in the DTMPP. The oxygen atom O33 is having short contact interaction with the hydrogen atom H44 with a distance of 3.3258 Å.
- Mulliken atomic charges uncover that all hydrogen atoms possess net positive charge but H40 atom has a more positive charge (0.131720) than other hydrogen atoms and thusly exceptionally acidic. The C14 atom has the most noteworthy net positive charge (0.258693) and the C16 is the most electronegative carbon (-0.172547).
- The MESP plot of the DTMPP proposes that the electrophilic attacks are feasible at both aromatic rings; However, ring C is more prone to the attack of electrophiles. The positive potential is around hydrogen atoms.
- The HOMO in the DTMPP is essentially situated at ring B and C. The LUMO is fundamentally arranged at the enone part of the unsaturated framework. The energy gap in the DTMPP is 3.783 eV which uncovers inescapable charge *transfer* phenomena occurring within the molecule.
- The absorption wavelength, oscillator strength, and *transitions* of DTMPP were computed at

TD-B3LYP/6-311++G(d,p) level of theory for B3LYP/6-311G ++(d,p) basis set. The UV-Visible spectrum was computed for six excited states. The first excited state absorption wavelength is 375.83 nm with excitation energy of 3.2990 eV and oscillator strength (f), 0.0035. With increase in the number of excited state, there is decrease in the absorption wavelength and increase in the excitation energy.

- The vibrational assignments for the DTMP were made by comparing the experimental IR spectrum with the theoretical IR spectrum. The DTMP contains 46 atoms; along these lines, it shows 132 fundamental modes of vibrations. The vibrational outcome shows that there is a perfect matching between experimental and theoretical vibrational peaks.
- E_{total} , heat capacity at constant volume, total entropy, zero point vibrational energy and rotational constants have been evaluated from harmonic vibrational frequencies.

Acknowledgments

Authors acknowledge Central instrumentation facility, Savitribai Phule Pune University, Pune for NMR and CIC, KTHM College, Nashik for FT-IR spectral analysis. Authors also would like to thank principal of Arts, Science and Commerce College, Manmad, for permission and providing necessary research facilities. Authors are very grateful to Prof. Arun B. Sawant for his generous help in the Gaussian study. Dr. Aapoorva Prashant Hiray, Coordinator, MG Vidyamandir Institute, is gratefully acknowledged for Gaussian package.

Funding

We have not received any kind of fund for the research work.

Conflict of Interest

Authors declared that he do not have any conflict of interest regarding this research article.

References

1. Li, J.T., Yang, W.Z., Wang, S.X., Li, S.H. and Li, T.S., 2002. Improved synthesis of chalcones under ultrasound irradiation. *Ultrasonics Sonochemistry*, 9(5), pp.237-239.
2. Eddarir, S., Cotelle, N., Bakkour, Y. and Rolando, C., 2003. An efficient synthesis of chalcones based on the Suzuki reaction. *Tetrahedron letters*, 44(28), pp.5359-5363.
3. Kumar, A., Sharma, S., Tripathi, V.D. and Srivastava, S., 2010. Synthesis of chalcones and flavanones using Julia-Kocienski olefination. *Tetrahedron*, 66(48), pp.9445-9449.
4. Jioui, I., Dâoun, K., Solhy, A., Jouiad, M., Zahouily, M., Essaid, B., Len, C. and Fihri, A., 2016. Modified fluorapatite as highly efficient catalyst for the synthesis of chalcones via Claisen-Schmidt condensation reaction. *Journal of Industrial and Engineering Chemistry*, 39, pp.218-225.
5. Adole, V.A., Jagdale, B.S., Pawar, T.B. and Sagane, A.A., 2020. Ultrasound promoted stereoselective synthesis of 2,3-dihydrobenzofuran appended chalcones at ambient temperature. *South African Journal of Chemistry*, 73, pp.35-43.
6. Rammohan, A., Reddy, J.S., Sravya, G., Rao, C.N. and Zyryanov, G.V., 2020. Chalcone synthesis, properties and medicinal applications: a review. *Environmental Chemistry Letters*, pp.1-26.
7. Yang, J.L., Ma, Y.H., Li, Y.H., Zhang, Y.P., Tian, H.C., Huang, Y.C., Li, Y., Chen, W. and Yang, L.J., 2019. Design, Synthesis, and Anticancer Activity of Novel Trimethoxyphenyl-Derived Chalcone-Benzimidazolium Salts. *ACS omega*, 4(23), pp.20381-20393.
8. Burmaoglu, S., Yilmaz, A.O., Polat, M.F., Kaya, R., Gulcin, İ. and Algul, O., 2019. Synthesis of novel tris-chalcones and determination of their inhibition profiles against some metabolic enzymes. *Archives of physiology and biochemistry*, pp.1-9.
9. Aljamali, N., Hamzah Daylee, S. and Jaber Kadhium, A., 2020. Review on Chemical-Biological Fields of Chalcone Compounds. *Forefront Journal of Engineering & Technology*, 2(1), pp.33-44.
10. Rozmer, Z. and Perjési, P., 2016. Naturally occurring chalcones and their biological

- activities. *Phytochemistry reviews*, 15(1), pp.87-120.
11. Yadav, L.D.S., Patel, R., Rai, V.K. and Srivastava, V.P., 2007. An efficient conjugate hydrothiocyanation of chalcones with a task-specific ionic liquid. *Tetrahedron letters*, 48(44), pp.7793-7795.
 12. MURAOKA, O., SAWADA, T., MORIMOTO, E. and TANABE, G., 1993. Chalcones as synthetic intermediates. A facile route to (\pm)-magnosalicin, an anti-allergy neolignan. *Chemical and pharmaceutical bulletin*, 41(4), pp.772-774.
 13. Kalirajan, R., Sivakumar, S.U., Jubie, S., Gowramma, B. and Suresh, B., 2009. Synthesis and biological evaluation of some heterocyclic derivatives of chalcones. *Int. J. ChemTech Res*, 1(1), pp.27-34.
 14. Elarfi, M.J. and Al-Difar, H.A., 2012. Synthesis of some heterocyclic compounds derived from chalcones. *Scientific Reviews and Chemical Communications*, 2(2), pp.103-107.
 15. MT Albuquerque, H., MM Santos, C., AS Cavaleiro, J. and MS Silva, A., 2014. Chalcones as Versatile Synthons for the Synthesis of 5- and 6-membered Nitrogen Heterocycles. *Current Organic Chemistry*, 18(21), pp.2750-2775.
 16. Kidwai, M. and Misra, P., 1999. Ring closure reactions of chalcones using microwave technology. *Synthetic communications*, 29(18), pp.3237-3250.
 17. Yadav, P., Lal, K., Kumar, A., Guru, S.K., Jaglan, S. and Bhushan, S., 2017. Green synthesis and anticancer potential of chalcone linked-1, 2, 3-triazoles. *European journal of medicinal chemistry*, 126, pp.944-953.
 18. Zhao, L., Mao, L., Hong, G., Yang, X. and Liu, T., 2015. Design, synthesis and anticancer activity of matrine-1H-1, 2, 3-triazole-chalcone conjugates. *Bioorganic & medicinal chemistry letters*, 25(12), pp.2540-2544.
 19. Rai, U.S., Isloor, A.M., Shetty, P., Pai, K.S.R. and Fun, H.K., 2015. Synthesis and in vitro biological evaluation of new pyrazole chalcones and heterocyclic diamides as potential anticancer agents. *Arabian Journal of Chemistry*, 8(3), pp.317-321.
 20. Madhavi, S., Sreenivasulu, R., Yazala, J.P. and Raju, R.R., 2017. Synthesis of chalcone incorporated quinazoline derivatives as anticancer agents. *Saudi Pharmaceutical Journal*, 25(2), pp.275-279.
 21. Mujahid, M., Yogeewari, P., Sriram, D., Basavanag, U.M.V., Díaz-Cervantes, E., Córdoba-Bahena, L., Robles, J., Gonnade, R.G., Karthikeyan, M., Vyas, R. and Muthukrishnan, M., 2015. Spirochromone-chalcone conjugates as antitubercular agents: synthesis, bio evaluation and molecular modeling studies. *RSC Advances*, 5(129), pp.106448-106460.
 22. Singh, A., Viljoen, A., Kremer, L. and Kumar, V., 2018. Synthesis and antimycobacterial evaluation of piperazyl-alkyl-ether linked 7-chloroquinoline-chalcone/ferrocenyl chalcone conjugates. *ChemistrySelect*, 3(29), pp.8511-8513.
 23. Chu, W.C., Bai, P.Y., Yang, Z.Q., Cui, D.Y., Hua, Y.G., Yang, Y., Yang, Q.Q., Zhang, E. and Qin, S., 2018. Synthesis and antibacterial evaluation of novel cationic chalcone derivatives possessing broad spectrum antibacterial activity. *European journal of medicinal chemistry*, 143, pp.905-921.
 24. Vazquez-Rodriguez, S., López, R.L., Matos, M.J., Armesto-Quintas, G., Serra, S., Uriarte, E., Santana, L., Borges, F., Crego, A.M. and Santos, Y., 2015. Design, synthesis and antibacterial study of new potent and selective coumarin-chalcone derivatives for the treatment of tenacibaculosis. *Bioorganic & medicinal chemistry*, 23(21), pp.7045-7052.
 25. Alam, M.S., Rahman, S.M. and Lee, D.U., 2015. Synthesis, biological evaluation, quantitative-SAR and docking studies of novel chalcone derivatives as antibacterial and antioxidant agents. *Chemical Papers*, 69(8), pp.1118-1129.
 26. Tang, X., Su, S., Chen, M., He, J., Xia, R., Guo, T., Chen, Y., Zhang, C., Wang, J. and Xue, W., 2019. Novel chalcone derivatives containing a 1, 2, 4-triazine moiety: design, synthesis, antibacterial and antiviral activities. *RSC advances*, 9(11), pp.6011-6020.
 27. Hameed, A., Abdullah, M.I., Ahmed, E., Sharif, A., Irfan, A. and Masood, S., 2016. Anti-HIV cytotoxicity enzyme inhibition and molecular docking studies of quinoline based chalcones as potential non-nucleoside

- reverse transcriptase inhibitors (NNRT). *Bioorganic chemistry*, 65, pp.175-182.
28. Wu, J.H., Wang, X.H., Yi, Y.H. and Lee, K.H., 2003. Anti-AIDS agents 54. A potent anti-HIV chalcone and flavonoids from genus *Desmos*. *Bioorganic & medicinal chemistry letters*, 13(10), pp.1813-1815.
29. Rizvi, S.U.F., Siddiqui, H.L., Johns, M., Detorio, M. and Schinazi, R.F., 2012. Anti-HIV-1 and cytotoxicity studies of piperidyl-thienyl chalcones and their 2-pyrazoline derivatives. *Medicinal Chemistry Research*, 21(11), pp.3741-3749.
30. Singh, P., Anand, A. and Kumar, V., 2014. Recent developments in biological activities of chalcones: a mini review. *European journal of medicinal chemistry*, 85, pp.758-777.
31. Wu, X., Wilairat, P. and Go, M.L., 2002. Antimalarial activity of ferrocenyl chalcones. *Bioorganic & medicinal chemistry letters*, 12(17), pp.2299-2302.
32. Li, R., Kenyon, G.L., Cohen, F.E., Chen, X., Gong, B., Dominguez, J.N., Davidson, E., Kurzban, G., Miller, R.E., Nuzum, E.O. and Rosenthal, P.J., 1995. In vitro antimalarial activity of chalcones and their derivatives. *Journal of medicinal chemistry*, 38(26), pp.5031-5037.
33. Domínguez, J.N., León, C., Rodrigues, J., de Domínguez, N.G., Gut, J. and Rosenthal, P.J., 2005. Synthesis and antimalarial activity of sulfonamide chalcone derivatives. *Il Farmaco*, 60(4), pp.307-311.
34. Hans, R.H., Guantai, E.M., Lategan, C., Smith, P.J., Wan, B., Franzblau, S.G., Gut, J., Rosenthal, P.J. and Chibale, K., 2010. Synthesis, antimalarial and antitubercular activity of acetylenic chalcones. *Bioorganic & medicinal chemistry letters*, 20(3), pp.942-944.
35. Lahsasni, S.A., Al Korbi, F.H. and Aljaber, N.A.A., 2014. Synthesis, characterization and evaluation of antioxidant activities of some novel chalcones analogues. *Chemistry Central Journal*, 8(1), pp.1-10.
36. Aly, M.R.E.S., Fodah, H.H.A.E.R. and Saleh, S.Y., 2014. Antiobesity, antioxidant and cytotoxicity activities of newly synthesized chalcone derivatives and their metal complexes. *European journal of medicinal chemistry*, 76, pp.517-530.
37. Wang, G., Xue, Y., An, L., Zheng, Y., Dou, Y., Zhang, L. and Liu, Y., 2015. Theoretical study on the structural and antioxidant properties of some recently synthesised 2, 4, 5-trimethoxy chalcones. *Food chemistry*, 171, pp.89-97.
38. Wan, Z., Hu, D., Li, P., Xie, D. and Gan, X., 2015. Synthesis, antiviral bioactivity of novel 4-thioquinazoline derivatives containing chalcone moiety. *Molecules*, 20(7), pp.11861-11874.
39. Zhou, D., Xie, D., He, F., Song, B. and Hu, D., 2018. Antiviral properties and interaction of novel chalcone derivatives containing a purine and benzenesulfonamide moiety. *Bioorganic & medicinal chemistry letters*, 28(11), pp.2091-2097.
40. Wang, Y.J., Zhou, D.G., He, F.C., Chen, J.X., Chen, Y.Z., Gan, X.H., Hu, D.Y. and Song, B.A., 2018. Synthesis and antiviral bioactivity of novel chalcone derivatives containing purine moiety. *Chinese Chemical Letters*, 29(1), pp.127-130.
41. Konduru, N.K., Dey, S., Sajid, M., Owais, M. and Ahmed, N., 2013. Synthesis and antibacterial and antifungal evaluation of some chalcone based sulfones and bisulfones. *European journal of medicinal chemistry*, 59, pp.23-30.
42. Parikh, K. and Joshi, D., 2013. Antibacterial and antifungal screening of newly synthesized benzimidazole-clubbed chalcone derivatives. *Medicinal Chemistry Research*, 22(8), pp.3688-3697.
43. Kulkarni, R.R., Tupe, S.G., Gample, S.P., Chandgude, M.G., Sarkar, D., Deshpande, M.V. and Joshi, S.P., 2014. Antifungal dimeric chalcone derivative kamalachalcone E from *Mallotus philippinensis*. *Natural product research*, 28(4), pp.245-250.
44. Zheng, Y., Wang, X., Gao, S., Ma, M., Ren, G., Liu, H. and Chen, X., 2015. Synthesis and antifungal activity of chalcone derivatives. *Natural product research*, 29(19), pp.1804-1810.
45. de Sá, N.P., Cisalpino, P.S., Tavares, L.D.C., Espíndola, L., Pizzolatti, M.G., Santos, P.C., de Paula, T.P., Rosa, C.A., de Souza, D.D.G., Santos, D.A. and Johann, S., 2015. Antifungal activity of 6-quinolinyl

- N-oxide chalcones against *Paracoccidioides*. *Journal of Antimicrobial Chemotherapy*, 70(3), pp.841-845.
46. Mahapatra, D.K. and Bharti, S.K., 2016. Therapeutic potential of chalcones as cardiovascular agents. *Life sciences*, 148, pp.154-172.
47. Opletalova, V., Jahodar, L., Jun, D. and Opletal, L., 2003. Chalcones (1, 3-diarylpropen-1-ones) and their analogs as potential therapeutic agents in cardiovascular system diseases. *Ceska a Slovenska farmacie: casopis Ceske farmaceuticke spolecnosti a Slovenske farmaceuticke spolecnosti*, 52(1), pp.12-19.
48. Kumar, S.K., Hager, E., Pettit, C., Gurulingappa, H., Davidson, N.E. and Khan, S.R., 2003. Design, synthesis, and evaluation of novel boronic-chalcone derivatives as antitumor agents. *Journal of medicinal chemistry*, 46(14), pp.2813-2815.
49. Kumar, D., Kumar, N.M., Akamatsu, K., Kusaka, E., Harada, H. and Ito, T., 2010. Synthesis and biological evaluation of indolyl chalcones as antitumor agents. *Bioorganic & medicinal chemistry letters*, 20(13), pp.3916-3919.
50. Xia, Y., Yang, Z.Y., Xia, P., Bastow, K.F., Nakanishi, Y. and Lee, K.H., 2000. Antitumor agents. Part 202: novel 2'-amino chalcones: design, synthesis and biological evaluation. *Bioorganic & medicinal chemistry letters*, 10(8), pp.699-701.
51. Sashidhara, K.V., Avula, S.R., Mishra, V., Palnati, G.R., Singh, L.R., Singh, N., Chhonker, Y.S., Swami, P. and Bhatta, R.S., 2015. Identification of quinoline-chalcone hybrids as potential antiulcer agents. *European journal of medicinal chemistry*, 89, pp.638-653.
52. Sharma, C.S., Shekhawat, K.S., Chauhan, C.S. and Kumar, N., 2013. Synthesis and anticonvulsant activity of some chalcone derivatives. *Journal of Chemical and Pharmaceutical Research*, 5(10), pp.450-454.
53. Singh, N., Ahmad, S. and Alam, M.S., 2012. Biological potentials of chalcones: a review. *International Journal of Pharmaceutical and Biological Archives*, 3(6), pp.1298-1303.
54. Mahapatra, D.K., Bharti, S.K. and Asati, V., 2017. Chalcone derivatives: Anti-inflammatory potential and molecular targets perspectives. *Current topics in medicinal chemistry*, 17(28), pp.3146-3169.
55. Bhale, P.S., Chavan, H.V., Dongare, S.B., Shringare, S.N., Mule, Y.B., Nagane, S.S. and Bandgar, B.P., 2017. Synthesis of extended conjugated indolyl chalcones as potent anti-breast cancer, anti-inflammatory and antioxidant agents. *Bioorganic & medicinal chemistry letters*, 27(7), pp.1502-1507.
56. Reddy, M.V.B., Hung, H.Y., Kuo, P.C., Huang, G.J., Chan, Y.Y., Huang, S.C., Wu, S.J., Morris-Natschke, S.L., Lee, K.H. and Wu, T.S., 2017. Synthesis and biological evaluation of chalcone, dihydrochalcone, and 1, 3-diarylpropane analogs as anti-inflammatory agents. *Bioorganic & medicinal chemistry letters*, 27(7), pp.1547-1550.
57. Wen, R., Lv, H.N., Jiang, Y. and Tu, P.F., 2018. Anti-inflammatory flavone and chalcone derivatives from the roots of *Pongamia pinnata* (L.) *Pierre. Phytochemistry*, 149, pp.56-63.
58. Wang, L., Yang, X., Zhang, Y., Chen, R., Cui, Y. and Wang, Q., 2019. Anti-inflammatory Chalcone-Isoflavone Dimers and Chalcone Dimers from *Caragana jubata*. *Journal of Natural Products*, 82(10), pp.2761-2767.
59. Nowakowska, Z., 2007. A review of anti-infective and anti-inflammatory chalcones. *European journal of medicinal chemistry*, 42(2), pp.125-137.
60. Makhlof, M.M., Radwan, A.S. and Ghazal, B., 2018. Experimental and DFT insights into molecular structure and optical properties of new chalcones as promising photosensitizers towards solar cell applications. *Applied Surface Science*, 452, pp.337-351.
61. Song, D.M., Jung, K.H., Moon, J.H. and Shin, D.M., 2003. Photochemistry of chalcone and the application of chalcone-derivatives in photo-alignment layer of liquid crystal display. *Optical Materials*, 21(1-3), pp.667-671.
62. Chaudhry, A.R., Irfan, A., Muhammad, S., Al-Sehemi, A.G., Ahmed, R. and Jingping, Z., 2017. Computational study of structural, optoelectronic and nonlinear optical properties of dynamic solid-state chalcone derivatives. *Journal of Molecular Graphics and Modelling*,

- 75, pp.355-364.
63. Ramaganthan, B., Gopiraman, M., Olasunkanmi, L.O., Kabanda, M.M., Yesudass, S., Bahadur, I., Adekunle, A.S., Obot, I.B. and Ebenso, E.E., 2015. Synthesized photo-cross-linking chalcones as novel corrosion inhibitors for mild steel in acidic medium: experimental, quantum chemical and Monte Carlo simulation studies. *RSC Advances*, 5(94), pp.76675-76688.
64. Indira, J., Karat, P.P. and Sarojini, B.K., 2002. Growth, characterization and nonlinear optical property of chalcone derivative. *Journal of crystal growth*, 242(1-2), pp.209-214.
65. Poornesh, P., Shettigar, S., Umesh, G., Manjunatha, K.B., Kamath, K.P., Sarojini, B.K. and Narayana, B., 2009. Nonlinear optical studies on 1, 3-disubstituent chalcones doped polymer films. *Optical materials*, 31(6), pp.854-859.
66. Shettigar, S., Chandrasekharan, K., Umesh, G., Sarojini, B.K. and Narayana, B., 2006. Studies on nonlinear optical parameters of bis-chalcone derivatives doped polymer. *Polymer*, 47(10), pp.3565-3567.
67. Ravindra, H.J., Kiran, A.J., Chandrasekharan, K., Shashikala, H.D. and Dharmaprakash, S.M., 2007. Third order nonlinear optical properties and optical limiting in donor/acceptor substituted 4'-methoxy chalcone derivatives. *Applied Physics B*, 88(1), pp.105-110.
68. Adole, V.A., Pawar, T.B., Koli, P.B. and Jagdale, B.S., 2019. Exploration of catalytic performance of nano-La₂O₃ as an efficient catalyst for dihydropyrimidinone/thione synthesis and gas sensing. *Journal of Nanostructure in Chemistry*, 9(1), pp.61-76.
69. Ritter, M., Martins, R.M., Rosa, S.A., Malavolta, J.L., Lund, R.G., Flores, A.F. and Pereira, C.M., 2015. Green synthesis of chalcones and microbiological evaluation. *Journal of the Brazilian Chemical Society*, 26(6), pp.1201-1210.
70. Rateb, N.M. and Zohdi, H.F., 2009. Atom-efficient, solvent-free, green synthesis of chalcones by grinding. *Synthetic Communications*, 39(15), pp.2789-2794.
71. Adole, V.A., Pawar, T.B. and Jagdale, B.S., 2019. Aqua-mediated rapid and benign synthesis of 1, 2, 6, 7-tetrahydro-8H-indeno [5,4-b] furan-8-one-appended novel 2-arylidene indanones of pharmacological interest at ambient temperature. *Journal of the Chinese Chemical Society*, 67:306-315.
72. Vieira, Lucas CC, Márcio Weber Paixão, and Arlene G. Corrêa. "Green synthesis of novel chalcone and coumarin derivatives via Suzuki coupling reaction." *Tetrahedron Letters* 53, no. 22 (2012): 2715-2718.
73. Romanelli, G., Pasquale, G., Sathicq, Á., Thomas, H., Autino, J. and Vázquez, P., 2011. Synthesis of chalcones catalyzed by aminopropylated silica sol-gel under solvent-free conditions. *Journal of Molecular Catalysis A: Chemical*, 340(1-2), pp.24-32.
74. Rani, M.S., Rohini, C., Keerthi, B.S. and Mamata, C., 2019. Green Synthesis of Novel Chalcone Derivatives, Characterization and its Antibacterial Activity. *Research Journal of Science and Technology*, 11(3), pp.183-185.
75. Adole, V.A., More, R.A., Jagdale, B.S., Pawar, T.B. and Chobe, S.S., 2020. Efficient Synthesis, Antibacterial, Antifungal, Antioxidant and Cytotoxicity Study of 2-(2-Hydrazineyl) thiazole Derivatives. *ChemistrySelect*, 5(9), pp.2778-2786.
76. Adole, V.A., Waghchaure, R.H., Jagdale, B.S. and Pawar, T.B., 2020. Investigation of Structural and Spectroscopic Parameters of Ethyl 4-(4-isopropylphenyl)-6-methyl-2-oxo-1,2,3,4-tetrahydropyrimidine-5-carboxylate: a DFT Study. *Chemistry & Biology Interface*, 10(1), 22-20.
77. Selvaraj, S., Rajkumar, P., Kesavan, M., Thirunavukkarasu, K., Gunasekaran, S., Devi, N.S. and Kumaresan, S., 2020. Spectroscopic and structural investigations on modafinil by FT-IR, FT-Raman, NMR, UV-Vis and DFT methods. *Spectrochimica Acta Part A: Molecular and Biomolecular Spectroscopy*, 224, p.117449.
78. Pallavi, L., Tonannavar, J. and Tonannavar, J., 2020. DFT zwitterion model for vibrational and electronic structure of unnatural 3-amino-3-(4-fluorophenyl) propionic acid, aided by IR and Raman spectroscopy. *Journal of Molecular Structure*, p.128085.
79. Ramesh, P., Caroline, M.L., Muthu, S.,

- Narayana, B., Raja, M. and Aayisha, S., 2020. Spectroscopic and DFT studies, structural determination, chemical properties and molecular docking of 1-(3-bromo-2-thienyl)-3-[4-(dimethylamino)-phenyl] prop-2-en-1-one. *Journal of Molecular Structure*, 1200, p.127123.
80. Iramain, M.A., Ledesma, A.E., Imbarack, E., Bongiorno, P.L. and Brandán, S.A., 2020. Spectroscopic studies on the potassium 1-fluorobenzoyltrifluoroborate salt by using the FT-IR, Raman and UV-Visible spectra and DFT calculations. *Journal of Molecular Structure*, 1204, p.127534.
81. Adole, V.A., Jagdale, B.S., Pawar, T.B. and Sawant, A.B., Experimental and theoretical exploration on single crystal, structural, and quantum chemical parameters of (E)-7-(arylidene)-1,2,6,7-tetrahydro-8H-indeno [5, 4-b] furan-8-one derivatives: A comparative study. *Journal of the Chinese Chemical Society*. <https://doi.org/10.1002/jccs.202000006>.
82. Raja, M., Muhamed, R.R., Muthu, S. and Suresh, M., 2017. Synthesis, spectroscopic (FT-IR, FT-Raman, NMR, UV-Visible), NLO, NBO, HOMO-LUMO, Fukui function and molecular docking study of (E)-1-(5-bromo-2-hydroxybenzylidene) semicarbazide. *Journal of Molecular Structure*, 1141, pp.284-298.
83. Raja, M., Muhamed, R.R., Muthu, S. and Suresh, M., 2017. Synthesis, spectroscopic (FT-IR, FT-Raman, NMR, UV-Visible), first order hyperpolarizability, NBO and molecular docking study of (E)-1-(4-bromobenzylidene) semicarbazide. *Journal of Molecular Structure*, 1128, pp.481-492.
84. Pathak, S.K., Srivastava, R., Sachan, A.K., Prasad, O., Sinha, L., Asiri, A.M. and Karabacak, M., 2015. Experimental (FT-IR, FT-Raman, UV and NMR) and quantum chemical studies on molecular structure, spectroscopic analysis, NLO, NBO and reactivity descriptors of 3, 5-Difluoroaniline. *Spectrochimica Acta Part A: Molecular and Biomolecular Spectroscopy*, 135, pp.283-295.
85. Abbas, A., Gökce, H., Bahçeli, S. and Naseer, M.M., 2014. Spectroscopic (FT-IR, Raman, NMR and UV-vis.) and quantum chemical investigations of (E)-3-[4-(pentyloxyphenyl)-1-phenylprop-2-en-1-one. *Journal of Molecular Structure*, 1075, pp.352-364.
86. Govindarasu, K., Kavitha, E. and Sundaraganesan, N., 2014. Synthesis, structural, spectral (FTIR, FT-Raman, UV, NMR), NBO and first order hyperpolarizability analysis of N-phenylbenzenesulfonamide by density functional theory. *Spectrochimica Acta Part A: Molecular and Biomolecular Spectroscopy*, 133, pp.417-431.
87. Karabacak, M., Bilgili, S., Mavis, T., Eskici, M. and Atac, A., 2013. Molecular structure, spectroscopic characterization (FT-IR, FT-Raman, UV and NMR), HOMO and LUMO analysis of 3-ethynylthiophene with DFT quantum chemical calculations. *Spectrochimica Acta Part A: Molecular and Biomolecular Spectroscopy*, 115, pp.709-718.
88. Ayeshamariam, A., Ramalingam, S., Bououdina, M. and Jayachandran, M., 2014. Preparation and characterizations of SnO₂ nanopowder and spectroscopic (FT-IR, FT-Raman, UV-Visible and NMR) analysis using HF and DFT calculations. *Spectrochimica Acta Part A: Molecular and Biomolecular Spectroscopy*, 118, pp.1135-1143.
89. Sachan, A.K., Pathak, S.K., Sinha, L., Prasad, O., Karabacak, M. and Asiri, A.M., 2014. A combined experimental and theoretical investigation of 2-Thienylboronic acid: Conformational search, molecular structure, NBO, NLO and FT-IR, FT-Raman, NMR and UV spectral analysis. *Journal of Molecular Structure*, 1076, pp.639-650.
90. Karabacak, M., Sinha, L., Prasad, O., Asiri, A.M., Cinar, M. and Shukla, V.K., 2014. FT-IR, FT-Raman, NMR, UV and quantum chemical studies on monomeric and dimeric conformations of 3, 5-dimethyl-4-methoxybenzoic acid. *Spectrochimica Acta Part A: Molecular and Biomolecular Spectroscopy*, 123, pp.352-362.
91. Thirunavukkarasu, K., Rajkumar, P., Selvaraj, S., Suganya, R., Kesavan, M., Gunasekaran, S. and Kumaresan, S., 2018. Vibrational (FT-IR and FT-Raman), electronic (UV-Vis), NMR (1H and 13C) spectra and molecular docking analyses of anticancer molecule 4-hydroxy-3-methoxycinnamaldehyde. *Journal of Molecular Structure*, 1173, pp.307-320.

92. Gokce, H., Bahceli, S., Akyildirim, O., Yuksek, H. and Kol, O.G., 2013. The Syntheses, Molecular Structures, Spectroscopic Properties (IR, Micro-Raman, NMR and UV-vis) and DFT Calculations of Antioxidant 3-alkyl-4-[3-methoxy-4-(4-methylbenzoyl)benzylideneamino]-4,5-dihydro-1H-1,2,4-triazol-5-one Molecules. *Letters in Organic Chemistry*, 10(6), pp.395-441.
93. Sas, E.B., Kose, E., Kurt, M. and Karabacak, M., 2015. FT-IR, FT-Raman, NMR and UV-Vis spectra and DFT calculations of 5-bromo-2-ethoxyphenylboronic acid (monomer and dimer structures). *Spectrochimica Acta Part A: Molecular and Biomolecular Spectroscopy*, 137, pp.1315-1333.
94. Deval, V., Kumar, A., Gupta, V., Sharma, A., Gupta, A., Tandon, P. and Kunimoto, K.K., 2014. Molecular structure (monomeric and dimeric) and hydrogen bonds in 5-benzyl 2-thiohydantoin studied by FT-IR and FT-Raman spectroscopy and DFT calculations. *Spectrochimica Acta Part A: Molecular and Biomolecular Spectroscopy*, 132, pp.15-26.
95. Ramalingam, S., Periandy, S., Sugunakala, S., Prabhu, T. and Bououdina, M., 2013. Insilico molecular modeling, docking and spectroscopic [FT-IR/FT-Raman/UV/NMR] analysis of Chlorfenson using computational calculations. *Spectrochimica Acta Part A: Molecular and Biomolecular Spectroscopy*, 115, pp.118-135.
96. Chamundeeswari, S.V., Samuel, E.J.J. and Sundaraganesan, N., 2014. Molecular structure, vibrational spectra, NMR and UV spectral analysis of sulfamethoxazole. *Spectrochimica Acta Part A: Molecular and Biomolecular Spectroscopy*, 118, pp.1-10.
97. Karthikeyan, N., Prince, J.J., Ramalingam, S. and Periandy, S., 2015. Electronic [UV-visible] and vibrational [FT-IR, FT-Raman] investigation and NMR-mass spectroscopic analysis of terephthalic acid using quantum Gaussian calculations. *Spectrochimica Acta Part A: Molecular and Biomolecular Spectroscopy*, 139, pp.229-242.
98. Xavier, S. and Periandy, S., 2015. Spectroscopic (FT-IR, FT-Raman, UV and NMR) investigation on 1-phenyl-2-nitropropene by quantum computational calculations. *Spectrochimica Acta Part A: Molecular and Biomolecular Spectroscopy*, 149, pp.216-230.
99. Shakila, G., Saleem, H. and Sundaraganesan, N., 2017. FT-IR, FT-Raman, NMR and UV Spectral investigation: Computation of vibrational frequency, chemical shifts and electronic structure calculations of 1-bromo-4-nitrobenzene. *World Scientific News*, 61(2), pp.150-185.
100. Vitnik, V.D. and Vitnik, Ž.J., 2015. The spectroscopic (FT-IR, FT-Raman, ¹³C, ¹H NMR and UV) and NBO analyses of 4-bromo-1-(ethoxycarbonyl) piperidine-4-carboxylic acid. *Spectrochimica Acta Part A: Molecular and Biomolecular Spectroscopy*, 138, pp.1-12.
101. Sas, E.B., Kurt, M., Karabacak, M., Poiyamozhi, A. and Sundaraganesan, N., 2015. FT-IR, FT-Raman, dispersive Raman, NMR spectroscopic studies and NBO analysis of 2-Bromo-1H-Benzimidazol by density functional method. *Journal of Molecular Structure*, 1081, pp.506-518.
102. Karabacak, M., Cinar, M., Kurt, M., Poiyamozhi, A. and Sundaraganesan, N., 2014. The spectroscopic (FT-IR, FT-Raman, UV and NMR) first order hyperpolarizability and HOMO-LUMO analysis of dansyl chloride. *Spectrochimica Acta Part A: Molecular and Biomolecular Spectroscopy*, 117, pp.234-244.